Research paper

Study on the Detonation Reaction-zone and Energy Release Characteristics of a Cast HMX-based PBX

Kaiyuan Tan,[1,2] **Yong Han,**[2] **Guan Luo,**[2] **Ming Yin,**[2] **Shanggang Wen,**[2] **Fenglei Huang**[1]

[1] *School of Mechatronic Engineering, Beijing Institute of Technology (BIT), Beijing 100081, China*
[2] *Institute of Chemical Materials, China Academy of Engineering Physics (CAEP), Mianyang 621999, Sichuan, China*

Abstract: This article gives a comprehensive study of the detonation reaction-zone (DRZ) and energy release characteristics of a cast HMX-based polymer-bonded explosive, PBX-91C, which has been demonstrated in our previous study to be an insensitive explosive. The DRZ of PBX-91C was studied by the impedance window method; the detonation reaction time, DRZ length, and detonation pressure were obtained. The cylinder test was employed to evaluate the acceleration ability of PBX-91C, the Gurney velocity and the parameters of the Jones-Wilkins-Lee (JWL) equation of state (EOS) for PBX-91C. The shock overpressure test was carried out to evaluate the energy release characteristics of PBX-91C in free-field; TNT was also tested for comparison. On the basis of the parameters of the JWL EOS determined by the cylinder test, three-dimensional numerical simulations of the shock overpressure tests were conducted. The results showed that PBX-91C is substantially more powerful than TNT; moreover, the energy release of PBX-91C is more rapid. All of these results suggest that the detonation performance of PBX-91C is close to that of RDX. PBX-91C can be a good candidate for main charges as it has both high energy and low sensitivity.

Keywords: cast polymer-bonded explosive, detonation reaction-zone, energy release characteristics, shock overpressure

1   Introduction

High explosive (HE) HMX is a solid energetic compound with the best comprehensive properties, such as excellent detonation performance and relatively good thermal stability [1-3]. Polymer-bonded explosives (PBXs) are highly filled composite materials, comprising an energetic compound as the main component held together by a small quantity of polymeric binder [4, 5]. The introduction of polymeric binders into an energetic compound, which is generally brittle, can confer lower vulnerability and better safety on the resulting PBX. Therefore, HMX-based PBXs hold the merits of both high energy and relatively low sensitivity, making them the preferred energetic materials for main charges to accelerate metals.

Evaluating the acceleration ability of main charges is an important way to study the energy release characteristics. It has been the subject of considerable experimental and theoretical interest [6, 7]. The acceleration ability of a main charge depends mainly on the energy released during detonation. According to the Zeldovich-Neumann-Doring (ZND) detonation model, the detonation wave consists of a shock wave propagating over the HE, which is followed by a chemical reaction zone terminated by a Chapman-Jouguet (CJ) plane. The DRZ, where most exothermic chemical reactions occur, thus plays a significant role in the energy release of explosives. The DRZ length is generally defined as the distance or time from the shock front (or named as the von Neumann peak) to the CJ state. A shorter DRZ length of an explosive indicates a shorter chemical reaction ending time and a more rapid energy release during its detonation. In the ideal situation, the DRZ length is zero, and the ZND detonation model returns to the classical CJ detonation model. After the chemical reactions have ended at the CJ state, the detonation products behind the DRZ expand backward (known as the Taylor rarefaction wave) and accelerate the surrounding matters.

Over recent decades, numerous experimental studies have been reported to determine the DRZ length of solid explosives [8-14]. In these studies, the impedance window experiment has been the most used method, which measures the velocity of thin metal foils located on the boundary of HE charges with transparent windows; the particle velocity of thin foils at the interface can reproduce many details of the DRZ of the detonated samples [14]. All of these studies have also shown that the DRZ length for common solid explosives is in the range of 10^{-2} to 1 mm (or 10^{-2} to 10^{-1} μs).

The cylinder test is a basic method for the experimental determination of the acceleration ability of a main charge [7, 15-16]. According to the method,

the sample is placed in a cylindrical metal shell and initiated on one end face; in this case, the acceleration ability of the sample is determined from the radial acceleration of the shell. The results of cylinder tests make it possible to determine the so-called Gurney energy (E_G) or Gurney velocity ($(2E_G)^{1/2}$), the widely used indicators of acceleration ability inferred by Gurney based on simple assumptions [17, 18]. However, the cylinder test usually gives the results of acceleration ability at the expansion rate (the specific volume (V/V_0)) of the detonation products as less than 10, which corresponds to the expansion distance on the scale of less than 100 mm. For longer expansion distances (more than 100 mm), the energy release characteristics of a main charge are usually evaluated by the shock overpressure test, which measures the shock pressure wave induced by the detonated sample in free-field. The measured shock overpressure and shock impulse data, obtained by integrating the pressure wave with respect to time, can be used to determine the relative blast performance of the sample at large expansion rates to that of a reference explosive (TNT is usually used) [19].

In the present research, a high solid-content cast HMX-based polymer-bonded explosive, PBX-91C, with HMX and the polymeric binder hydroxyl terminated polybutadiene (HTPB) in a ratio of 90 wt.%/10 wt.%, was prepared as a candidate for the main charge. Our previous studies have shown that PBX-91C is an insensitive explosive with good safety [20, 21]. In present article, we focus on its detonation performance, hence the DRZ length, the acceleration ability, and the shock overpressure of PBX-91C in free-field, were investigated by experimental and numerical methods. The objective here was to make a comprehensive study of the DRZ and the energy release characteristics of the main charge candidate.

# 2   Experimental

2.1 Sample preparation

The cast HMX-based PBX (PBX-91C) was prepared with the solid HMX (Gansu Yinguang Chemical Industry Co. Ltd., China) and the polymeric binder HTPB (Liming Research and Design Institute of Chemical Industry Co. Ltd., China) in a mass ratio of 90%/10%. The HMX particles (with an average size of about 300 μm) and liquid HTPB were mixed for 30 min at 50 °C, followed by vacuum mixing for a further 30 min to drive out entrapped air, and the mixture was then cast and cured at 65 ±2 °C for five days under vacuum. The initial densities of the prepared samples were measured by floatation.

2.2 Detonation performance measurements

Detonation velocity, D_{CJ}, was measured by the electrical shorting pin method; mean values of three measurements (max. ±0.08 km·s^{-1}) were used. The DRZ of PBX-91C was studied by the impedance window method with the help of a Photon Doppler velocimetry (PDV) system [22]. As shown in Figure 1, the cylindrical sample was directly initiated from one end face by an electric detonator, and a PDV probe was used to measure the velocity of a thin aluminum coating (about 1 μm thick) located at the interface between the other end face of the sample and a transparent lithium fluoride (LiF) window. The sample and window were joined closely together by a fixing clip, a drop of silicon oil being added to the interface to drive out entrapped air. The cylinder test (as shown in Figure 2) was employed to evaluate the acceleration ability of the explosives. The PBX-91C sample was confined in a copper tube (25.4 mm inner diameter and 2.54 mm wall thickness) and initiated from one end using an electric detonator. The introduction of the explosive cylinder into the copper tube requires leaving a gap between the two pieces. This gap was constant and equal to 0.2 mm. To avoid jet formation between the cylinder and the tube, the gap was filled with an epoxy-based pad. The radial expansion history of the copper wall was recorded by a high speed streak camera (SJZ-15). Oxygen free high conductivity copper (Cu-OFHC) was used for the tube material because of its high ductility, in order to allow large expansions without cracking. As shown in Figure 3, the shock overpressure induced by the detonated samples in free-field was measured by pressure sensors (PCB-137B22B). The bare cylindrical sample was placed on a wooden support at a height of 1.4 m and initiated by an electrical detonator no. 8. The distances between the center of the sample and the sensors (Sensor 1, Sensor 2, and Sensor 3) were 1.0, 1.5 and 2.0 m, respectively. Table 1 lists the details for the three kinds of tests. The mean values of two measurements for each kind of test were finally accepted.
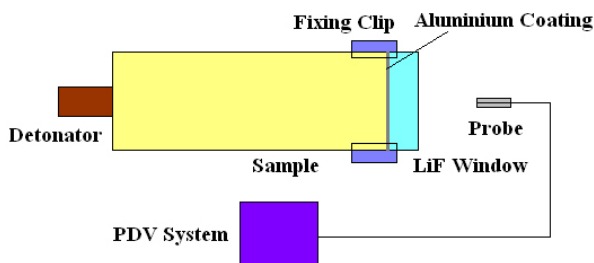
Figure 1   Schematic diagram of the arrangement for studying the DRZ of HE samples by the impedance window method
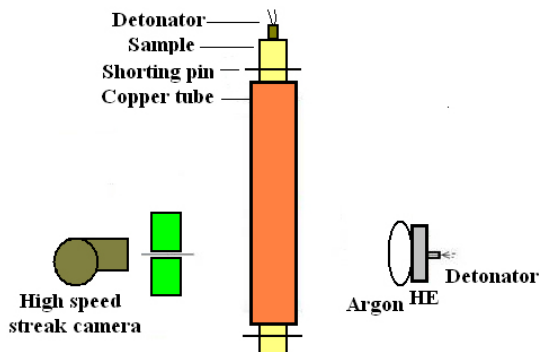
Figure 2. Schematic diagram of the arrangement for determining the acceleration ability by the cylinder test
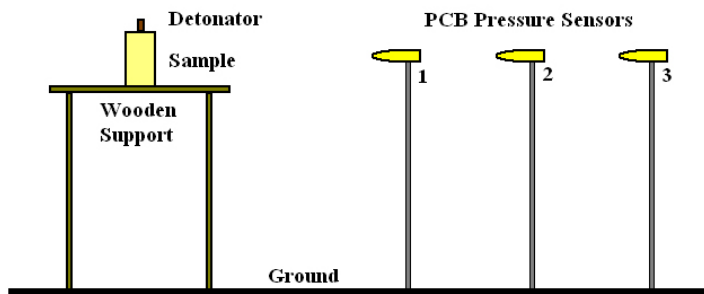
Figure 3. Schematic diagram of the arrangement for measuring the shock overpressure of the detonated samples by the pressure sensors

Table 1. Details of the tests

| Method	Size of samples [mm]	Density of samples [g·cm^{-3}]	Thickness of window/shell [mm]	Density of window/shell [g·cm^{-3}]
The DRZ test	Φ30 × 90		5.0	2.64
The cylinder test	Φ25.0 × 300	1.72	2.54	8.93
The shock overpressure test	Φ60 × 120		N.A.	N.A.

3   Results and Discussion

3.1 Detonation reaction zone structures

Figure 4 shows the particle velocity (u_p) profile of the HE-LiF interface for the PBX-91C sample. A chemical spike with a maximum (u_p) of ~2300 km·s^{-1} was recorded by the PDV system. The u_p dropped rapidly to ~1600 m·s^{-1} within approximately 100 ns, indicating a rapid chemical energy release in the DRZ. The u_p then decreased in a relatively slower way to ~1400 m·s^{-1} in the following 500 ns, indicating a relatively slower internal energy release of the detonation products due to their expansion in the Taylor rarefaction wave. However, it was difficult to distinguish directly an exact point on the profile of the particle velocity that corresponded to the CJ state which separated the DRZ and the Taylor rarefaction wave. In this study, we determined the position of the CJ state based on the first order derivative curve of the interface particle velocity (du_p/dt). Figure 5 shows the curve of du_p/dt *versus* time (t), before differentiation; the experimental profile of $u_p(t)$ was smoothed by the Savitzky-Golay method.
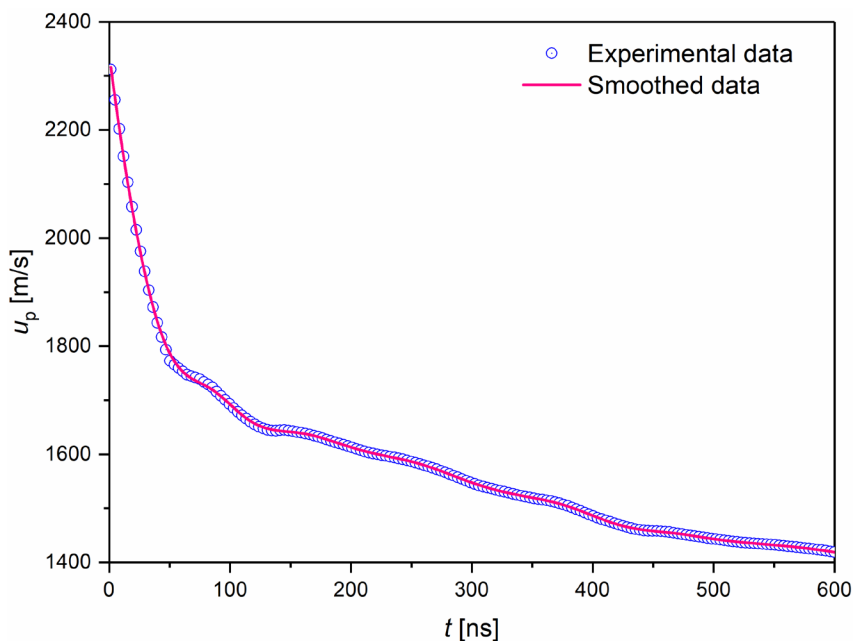
Figure 4.   Particle velocity (u_p) profile of the HE-LiF interface for the PBX-91C sample
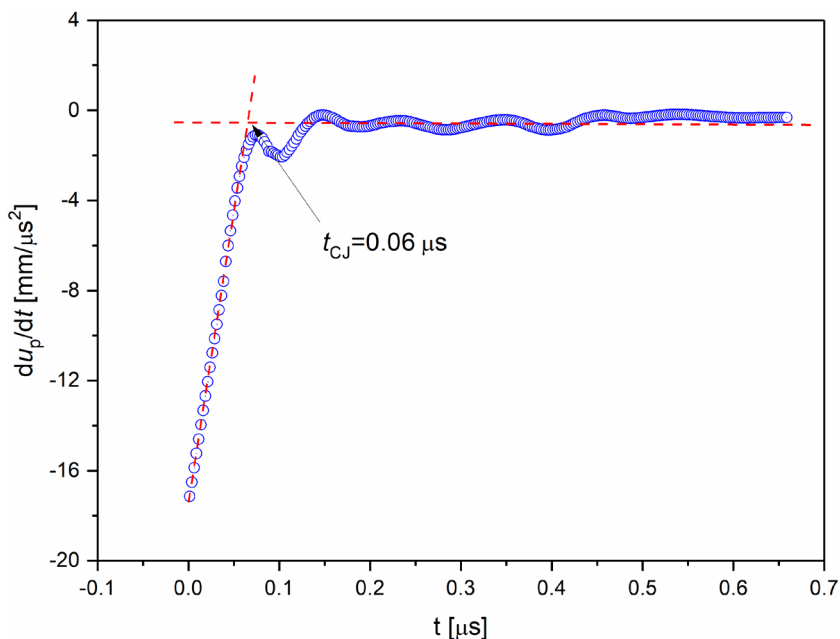
Figure 5.   First order derivative of the particle velocity *versus* time (du_p/dt) for PBX-91C

It was found from Figure 5 that the du_p/dt profile can be represented by two straight lines: one with a steep slope implying a sharp decrease of u_p in the DRZ, the other line with a practically zero slope implying a relatively constant and slow decrease of u_p in the Taylor wave region. The point of intersection of these two lines determines the reaction time (t_{CJ}) from the von Neumann peak to the CJ state. From Figure 5, a value of $t_{CJ} = 0.06$ μs was determined for the PBX-91C sample. The DRZ length (X_{CJ}) can be calculated from the following Equation 1 [11]:

$$X_{CJ} = \int_0^{t_{CJ}} (D_{CJ} - u_p)dt \tag{1}$$

where D_{CJ} is the detonation velocity; $D_{CJ} = 8.42$ km·s^{-1} was measured for PBX-91C by the electrical shorting pins method. Based on the $u_p(t)$ data in Figure 4, $X_{CJ} = 0.38$ mm was calculated for the PBX-91C sample.

The detonation pressure P_{CJ} can be estimated by the following Equation 2 [23]:

$$P_{CJ} = \frac{1}{2}u_{pCJ}[\rho_{W0}(5.15 + 1.35u_{PCJ}) + \rho_0 D_{CJ}] \tag{2}$$

where u_{pCJ} is the particle velocity at the CJ state; the value of u_{pCJ} can be determined as 1.76 km·s^{-1} when t_{CJ} = 0.06 μs; ρ_{W0} and ρ_0 are the initial densities of the LiF window and the HE sample, respectively; in this study, ρ_{W0} = 2.64 g·cm^{-3} and ρ_0 = 1.72 g·cm^{-3}. Thus, P_{CJ} = 30.2 GPa was calculated by Equation 2 for PBX-91C.

Table 2 summarizes the parameters of the DRZ for the PBX-91C sample and some common HEs. It can be found from Table 2 that the DRZ length of PBX-91C is much shorter than that of TNT, slightly longer than that of HMX, and closely comparable to that of RDX. These data suggest that, compared with common HEs as main charges, PBX-91C has a relatively narrow DRZ and can be regarded as an ideal explosive.

Table 2   Summary of the parameters of the DRZ for PBX-91C and some other common HEs [11]

High explosive	ρ_0/ρ_{max} [%]	t_{CJ} [μs]	X_{CJ} [mm]
PBX-91C	98.6	0.06 ±0.01	0.38 ±0.07
TNT(cast)	94.3	0.29 ±0.04	1.36 ±0.19
RDX	92.4	0.07 ±0.01	0.36 ±0.07
HMX	97.1	0.04 ±0.01	0.25 ±0.04

3.2 Acceleration ability

Cylinder test results are the basis for the determination of the acceleration ability and energetic characteristics of the detonation products of the PBX to be investigated. A typical photograph of the cylinder wall expansion process, recorded by a high speed streak camera, is shown in Figure 6.

Figure 6.   Typical photograph of the cylinder expansion process recorded by a high speed streak camera

The relation between the radial expansion distance of the cylinder $(R\text{-}R_0)$, in mm, and the expansion time (t), in μs, can be fitted by the following Equation 3:

$$t = a + b(R - R_0) + c\,\exp[d(R - R_0)] \tag{3}$$

where a, b, c and d are the fitting coefficients. The cylinder expansion velocity (u_m) can be obtained by differentiating Equation 3:

$$u_m = \frac{1}{b + cd\,\exp[d(R - R_0)]} \tag{4}$$

Based on the radial expansion history of the cylinder wall recorded by the high speed streak camera, the values of the fitting coefficients were determined as: $a = 2.24$, $b = 0.60$, $c = -1.55$, $d = -0.134$.

Generally, the acceleration ability of an explosive can be described by the Gurney energy or Gurney velocity $((2E_G)^{1/2})$. In the Gurney model, the $(2E_G)^{1/2}$ for some simple geometries filled with explosives is expressed as [17, 18]:

$$\sqrt{2E_G} = u_m\left(\alpha + \frac{n}{n+2}\right)^{\frac{1}{2}} \tag{5}$$

where u_m is the velocity of the metal, α is the ratio of the mass of metal (M) to the mass of explosive (m); $n = 1$ for the plane symmetric sandwich geometry, $n = 2$ for the cylindrical system, $n = 3$ for the spherical geometry. The velocity of the copper wall, u_m, at 19 mm displacement (which corresponded to a volume expansion of $V/V_0 = 7$) was determined by Equation 4, and the value of u_m was then used for calculation of the Gurney velocity using Equation 5. Table 3 shows the data of Gurney velocity, detonation velocity and detonation pressure for PBX-91C; the parameters for some other common HEs according to available literature data are also listed for comparison. It can be seen that the acceleration ability of PBX-91C is much higher than that of TNT, lower than that of HMX, and close to that of RDX.

Table 3. The data of Gurney velocity, detonation velocity and detonation pressure for PBX-91C and some other common HEs [18, 24]

High explosive	ρ_0 [g·cm^{-3}]	$(2E_G)^{1/2}$ [km·s^{-1}]	D_{CJ} [km·s^{-1}]	P_{CJ} [GPa]
PBX-91C	1.72	2.75 ±0.03[a]	8.42 ±0.08	30.2 ±0.6
TNT	1.63	2.37[a]	6.93	21.0
RDX	1.77	2.83[a]	8.70	33.8
HMX	1.89	2.97[a]	8.90	39.0

[a] At a volume expansion of $V/V_0 = 7$

The results of the cylinder test can also be used to determine the JWL EOS parameters of the detonation products. The JWL EOS is described as [25-27]:

$$p = A(1 - \frac{\omega}{R_1 v})\exp(-R_1 v) + B(1 - \frac{\omega}{R_2 v})\exp(-R_2 v) + \frac{\omega E_0}{v} \tag{6}$$

where p is the pressure of the detonation products (in Megabars), v is the relative volume, E_0 is the specific internal energy per unit mass of the explosive; A, B, R_1, R_2, and ω are the parameters to be determined, and which need to satisfy the measured CJ state, the measured expansion behaviour in the cylinder test, and some other conditions [28]. In the present study, the expansion process of the cylinder wall was numerically simulated by the Ansys/Ls-Dyna program, the MAT_HIGH_EXPLOSIVE_BURN and the MAT_JOHNSON_COOK were used as the material model for the explosive and copper wall, respectively, the EOS_JWL and the EOS_GRUNEISEN were used as the EOS for the explosive and copper wall, respectively. The parameters of JWL EOS for the sample were obtained by adjusting the numerical simulation results according to the experimental data. Here, the values of the JWL EOS parameters for PBX-91C were eventually determined as: $A = 6.9$, $B = 8 \cdot 10^{-2}$, $R_1 = 4.3$, $R_2 = 1.3$ and $\omega = 0.3$. Table 4 lists some values of the parameters used in the simulations. Figure 7 shows the simulated radial expansion history of the cylinder wall. It is obvious that the simulation results agree very well with the experimental data.

Table 4.   Some values of the parameters used in the simulation of the cylinder test

Material	Density [g·cm⁻³]	EOS_JWL parameters					
		A [Mbar]	B [Mbar]	R_1	R_2	ω	E_0 [Gerg/mm³]
PBX-91C	1.72	6.9	$8 \cdot 10^{-2}$	4.3	1.3	0.30	0.097

Material	Density [g·cm⁻³]	Young modulus [Mbar]	Shear modulus [Mbar]	Poisson ratio	EOS_GRUNEISEN parameters		
					Parameter C1 [cm/μs]	Parameter S1	Gruneisen coefficient
Copper	8.93	1.17	0.47	0.35	0.394	1.489	1.99
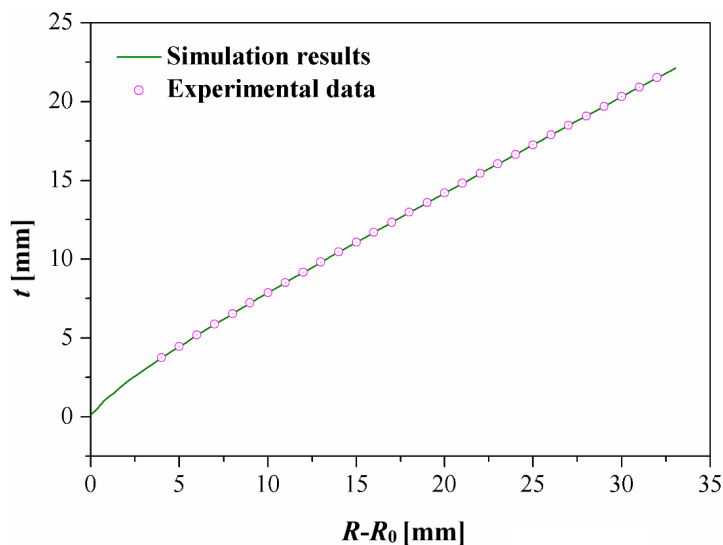
Figure 7.   Simulation results of the cylinder expansion history compared with experimental data

3.3 Energy release characteristics in free-field

The energy release characteristics of the samples in free-field (the expansion distance on a scale of more than 10^2 mm) were evaluated by the shock overpressure tests. On the basis of the JWL EOS parameters obtained by the cylinder tests (the parameters for TNT are available in [24]), three-dimensional numerical simulations of the shock overpressure tests were performed using the Ansys/Ls-Dyna software in order to gain a better understanding of the energy release characteristics of the samples. In these simulations, MAT_HIGH_EXPLOSIVE_BURN and MAT_NULL were used as the material models for the explosive and the air, respectively, and EOS_JWL and EOS_LINEAR_POLYNOMIAL were used as the equations of state for the explosive and the air, respectively. The linear polynomial EOS is given by:

$$p = C_0 + C_1\mu + C_2\mu^2 + C_3\mu^3 + (C_3 + C_5\mu + C_6\mu^2)E \tag{7}$$

in which p is the pressure, C_0, C_1, C_2, C_3, C_4, C_5 and C_6 are constants, E is the internal energy per initial volume and $\mu = 1/v - 1$. Table 5 lists some values of the parameters used in the simulations of the shock overpressure test. Figure 8 shows the simulated contours of the shock pressure at different expansion distances.

Table 5. Some values of the parameters used in the simulation of the shock overpressure test
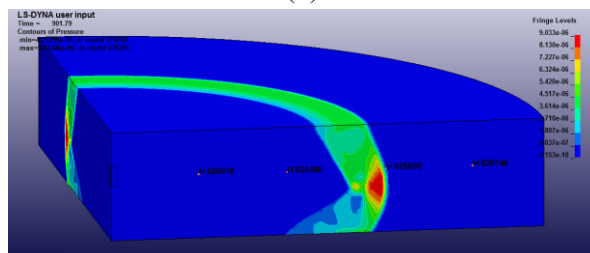
Material	Density [g·cm^{-3}]	EOS_JWL parameters					
		A [Mbar]	B [Mbar]	R_1	R_2	ω	E_0 [Gerg/mm^3]
PBX-91C	1.72	6.9	$8 \cdot 10^{-2}$	4.3	1.3	0.30	0.097
TNT	1.63	3.74	$7.33 \cdot 10^{-2}$	4.15	0.95	0.30	0.07

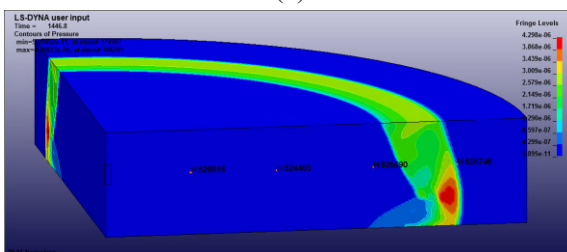| Material	Density [g·cm^{-3}]	EOS_LINEAR_POLYNOMIAL parameters						
		C_0 [Mbar]	C_1	C_2	C_3	C_4	C_5	C_6
Air	$1.29 \cdot 10^{-3}$	$1 \cdot 10^{-7}$	0	0	0	0.4	0.4	0
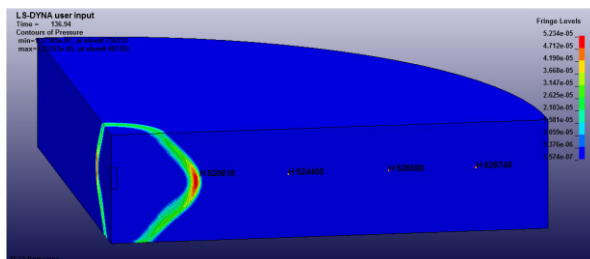
(a)
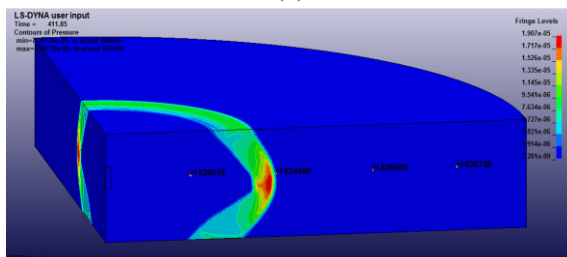
(b)

(c)

(d)

Figure 8.   The simulated contours of the shock overpressure at different expansion distances: (a) 0.5 m; (b) 1.0 m; (c) 1.5 m; (d) 2.0 m

Figure 9 shows the simulation results of the shock overpressure tests compared with the experimental data. It can be seen that the simulated

shock profiles at different distances agree quite well with the corresponding experimental ones. This means that the JWL EOS parameters determined by the cylinder tests are also applicable to the numerical simulations of the shock overpressure tests in free-field.
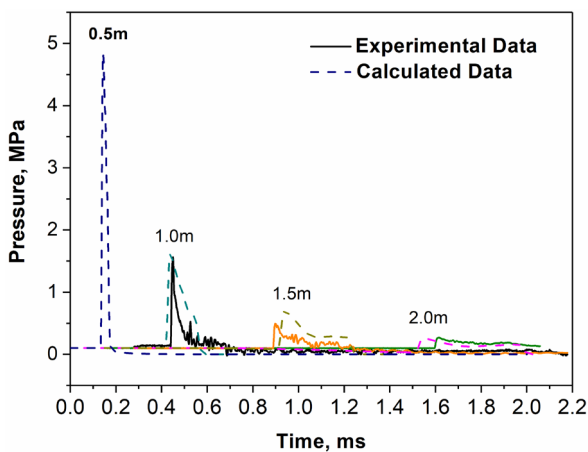

(a)
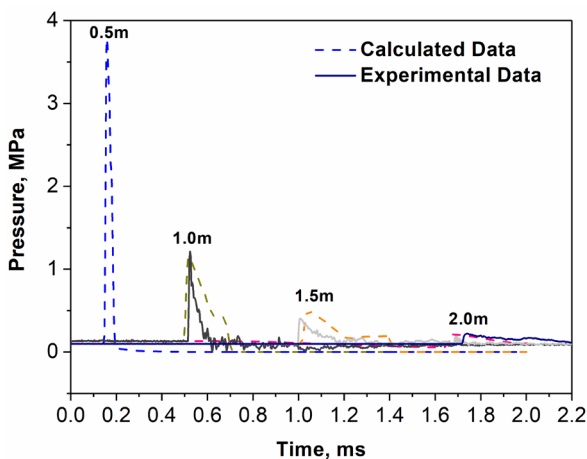
(b)

Figure 9. The simulation results of the shock overpressure test, compared with the experimental data: (a) PBX-91C; (b) TNT

Figure 10(a) draws a comparison between the simulation results of the shock profiles for PBX-91C and TNT. It can be found from Figure 10(a) that, at the same distance, the shock wave induced by the detonated PBX-91C sample

arrived earlier than that induced by the detonated TNT sample, due to the fact that the detonation velocity of PBX-91C is higher than that of TNT. Generally, the power of a shock wave can be mainly evaluated by two parameters:

1) the shock overpressure Δp, $\Delta p = p - p_0$, where p_0 is the atmospheric pressure, approximately 0.1 MPa, and
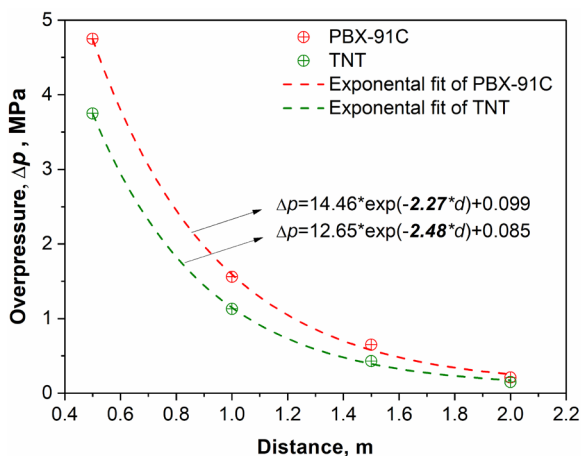
2) the shock impulse i, here $i = \int \Delta p dt$.

According to the data in Figure 10(a), at the same distance, the shock overpressure (Δp) and shock impulse (i) for PBX-91C are at least 20% and 10% higher than those for the TNT, respectively, indicating that PBX-91C is substantially more powerful than TNT in free-field.
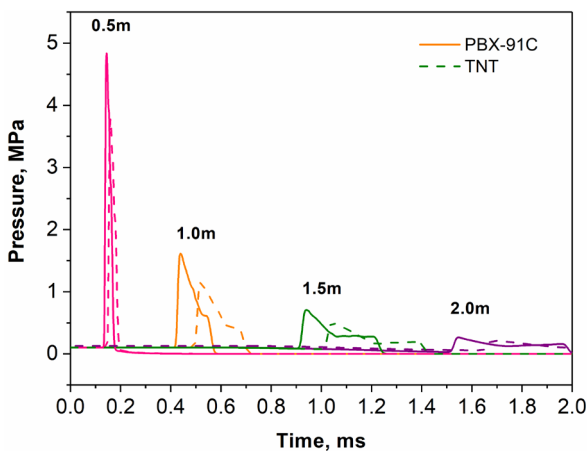
(a)
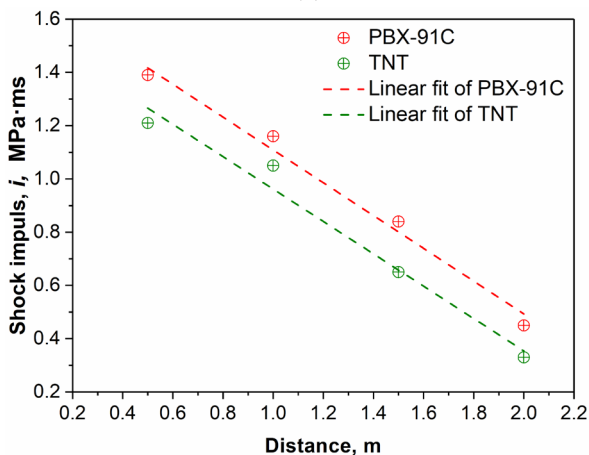
(b)

(c)

Figure 10. Comparisons between: (a) the simulation results of the shock profiles for PBX-91C and TNT; (b) the shock impulse attenuation laws for the detonated PBX-91C and TNT; (c) the shock overpressure attenuation laws for the detonated PBX-91C and TNT

It is also found from Figure 10(a) that the shock pressure of both PBX-91C and TNT decreases rapidly as the shock wave travels to longer distances, however, the shock duration increases. A further analysis of the data shows that the shock impulse, i, for both PBX-91C and TNT decreases linearly as the distance increases (as shown in Figure 10(b)), while the shock overpressure, Δp, decreases with the distance according to the exponential decay laws. As shown in Figure 10(c), the larger value of the decay exponent for PBX-91C indicates the faster attenuation of the Δp in this case; when the distance is 2 m, the difference between the overpressure of PBX-91C and TNT is less than 0.1 MPa. All of these results suggest that PBX-91C is more powerful than TNT. Moreover, the energy release of PBX-91C due to the expansion of the detonation products is more rapid.

4   Conclusions

A comprehensive study of the detonation reaction-zone (DRZ) structures and energy release characteristics of PBX-91C, a cast HMX-based polymer-bonded explosive with low sensitivity, is presented.

The DRZ of PBX-91C was studied by measuring the particle velocity at the detonated sample/LiF interface using a laser interferometer. The detonation reaction time $t_{CJ} = 0.06 \pm 0.01$ μs, DRZ length $X_{CJ} = 0.38 \pm 0.07$ mm, and detonation pressure $P_{CJ} = 30.2 \pm 0.6$ GPa were obtained.

The acceleration ability of PBX-91C was evaluated by the cylinder test, and the Gurney velocity $(2E_G)^{1/2} = 2.75 \pm 0.03$ km·s^{-1} (at $V/V_0 = 7$) was determined. The cylinder test was numerically simulated by the use of the Ls-Dyna program, and the parameters of the JWL EOS for PBX-91C were obtained by adjusting the numerical simulation results of the cylinder test according to the experimental data.

The free-field energy release characteristics of PBX-91C were evaluated by the shock overpressure test; TNT was also tested for comparison. On the basis of the parameters of the JWL EOS determined by the cylinder test, three-dimensional numerical simulation of the shock overpressure test was conducted. It was shown that the shock overpressure induced by the detonated PBX-91C was at least 20% higher than that induced by TNT. Moreover, the energy release of PBX-91C was more rapid.

All of these results suggest that the detonation performance of PBX-91C is close to that of RDX, and that PBX-91C is a good candidate for main charges as it has both high energy and low sensitivity.

References

[1] Gibbs, T.R.; Popolato, A. *LASL Explosive Property Data*. University of California Press, Berkeley, CA, **1980**.

[2] Xiao, H.M. *Structures and Properties of Energetic Compounds* (in Chinese). National Defense Industry Press, Beijing, China, **2004**.

[3] Zhang, C.Y.; Peng, Q.; Wang, L.; Wang, X. Thermal Sensitivity of HMX Crystals and HMX-Based Explosives Treated under Various Conditions. *Propellants Explos. Pyrotech*. **2010**, *35*: 561-566.

[4] Agrawal, J. *High Energy Materials: Propellants, Explosives and Pyrotechnics*. John Wiley & Sons, **2010**; ISBN 978-3-527-32610-5.

[5] Elbeih, A.; Wafy, T.Z.; Elshenawy, T. Performance and Detonation Characteristics of Polyurethane Matrix Bonded Attractive Nitramines. *Cent. Eur. J. Energ. Mater.* **2017**, *14*(1): 77-89.

[6] Li, J.S. A New Method for Evaluating the Energy Characteristics of C-H-N-O Energetic Compounds. *Propellants Explos. Pyrotech*. **2010**, *35*: 182 -185.

[7] Gogulyaa, M.F.; Brazhnikova, M.A.; Makhov, M.N.; Dolgoborodov, A.Y.; Lyubimov, A.V.; Sokolova, I.L. Effect of Aluminum on the Acceleration Ability

of Composite Formulations Based on Regular High Explosives. *Russ. J. Phys. Chem. B* **2012**, *6*(6): 730-743.

[8] Duff, R.E.; Houston, E. Measurement of Chapman Jouguet Pressure and Reaction Zone Length in a Detonating High Explosive. *J. Chem. Phys.* **1955**, *23*(7): 1268-1273.

[9] Gatilov, L.A.; Ibragimov, R.A.; Kudashov, A.V. Detonation Wave Structure in Cast TNT. *Combust. Explos. Shock Waves* **1989**, *25*(2): 82-84.

[10] Erskine, D.J.; Green, L.; Tarver, C.M. VIZAR Wave Profile Measurements in Supracompressed HE. In: *Shock Compression of Condensed Matter* (Schmidt, S.C.; Johnson, J.N.; Davison, L.W., Eds.), Elsevier, Amsterdam, **1990**, 717-720.

[11] Loboiko, B.G.; Lubyatinsky, S.N. Reaction Zones of Detonating Solid Explosives. *Combust. Explos. Shock Waves* **2000**, *36*(6): 716-733.

[12] Frank, A.; Chau, H.; Lee, R.; Vitello, P.; Souers, P.C. Reaction Zones in Ultrafine TATB. *Propellants Explos. Pyrotech.* **2003**, *28*(5): 259-264.

[13] Ershov, A.P.; Satonkina, N.P. Investigation of the Reaction Zone in Heterogeneous Explosives Substances Using an Electrical Conductivity Method. *Combust. Explos. Shock Waves* **2009**, *45*(2): 205-210.

[14] Utkin, A.; Mochalova, V. Detonation Wave Parameters of PETN and CL-20. *Int. Det. Symp.*, *Proc., 15th,* San Francisco, USA, **2014**.

[15] Reaugh, J.E.; Souers, P.C. A Constant-density Gurney Approach to the Cylinder Test. *Propellants Explos. Pyrotech.* **2004**, *29*(2): 124-128.

[16] Martin, K.; Jakub, S.; Jiri, P. First Attempts in Cylinder Expansion Testing. *New Trends Res. Energ. Mater., Proc. Semin., 20th,* Czech Republic, **2017**.

[17] Gurney, R.W. *The Initial Velocities of Fragments from Bombs, Shells and Grenades.* Ballistic Research Laboratory report 405, Aberdeen, Maryland, **1943**.

[18] Kennedy, J.E. The Gurney Model of Explosive Release for Driving Metal. *Explos. Eff. Appl.* **1998**, 221-257.

[19] Lee, R.J.; Felts, J.E.; Williams, J.H.; Woodworth, B. Comparison of Small-scale Tunnel and Large-scale Free-field Blast Performance. *Int. Det. Symp.*, *Proc., 15th,* San Francisco, USA, **2014**.

[20] Yin, M.; Luo, G.; Dai, X.G.; Zhang, P.J.; Tang, Y. Cook-off Test Investigation of High Solid-content Casted PBX Based on HMX (in Chinese). *Chin. J. Explos. Propellants* (*Huozhayao Xuebao*) **2014**, *37*(1): 44-48.

[21] Yin, M.; Luo, G.; Zheng, B.H.; Tang, Y.; Liu, X.W.; Dai, X.G.; Han, Y.; Huang, H.; Wu, K.X. Design and Performance of an Insensitve Cast PBX with High Gurney Energy (in Chinese). *Chin. J. Energ. Mater.* (*Hanneng Cailiao*) **2014**, *22*(4): 487-492.

[22] Briggs, M.E.; Hill, L.G.; Hull, L.M.; Shinas, M.A. Applications and Principles of Photon Doppler Velocimetry for Explosive Testing. *Int. Det. Symp.*, *Proc., 14th,* Coeur d'Alene, Idaho, **2010**.

[23] Liu, D.Y.; Chen, L.; Wang, C.; Zhang, L.S. Detonation Reaction-Zone Structure of CL-20. (in Chinese) *Nat. Symp. Explos. Mech., Proc., 10th,* Guiyang, China. **2014**, 325-329.

[24] Dobratz, B.M.; Crawford, P.C. *LLNL Explosives Handbook, Properties of Chemical Explosives and Explosive Simulants.* UCRL-52997 Rev. 2, Livermore, CA, **1985**.

[25] Baudin, G.; Serradeill, R. Review of Jones-Wilkins-Lee Equation of State. *Eur. Phys. J. Conf., Proc., 10th,* **2010**.

[26] Sanchidrian, J.A.; Castedo, R.; Lopez, L.M.; Segarra, P.; Santos, A.P. Determination of the JWL Constants for ANFO and Emulsion Explosives from Cylinder Test Data. *Cent. Eur. J. Energ. Mater.* **2015**, *12*(2): 177-194.

[27] Trzciński, W.A.; Szymańczyk, L.; Kramarczyk, B. Determination of the Equation of State for the Detonation Products of Emulsion Explosives. *Cent. Eur. J. Energ. Mater.* **2019**, *16*(1): 49-64.

[28] Elbeih, A.; Elshenawy, T.; Zeman, S.; Aksten, Z. Application of BCHMX in Shaped Charges against RHA Targets Compared to Different Nitramine Explosives. *Cent. Eur. J. Energ. Mater*. **2018**, *15*(1): 3-17.